

## Structural Studies on Optical Resolution *via* Diastereoisomeric Salt Formation, Part 2. The Conformational Flexibility of (*S*)-2-Benzylaminobutan-1-ol in Enantiomer Separation for Permethrinic Acids

Kálmán Simon,\* Éva Kozsda, and Zsolt Böcskei

CHINOIN Pharmaceutical and Chemical Works Ltd., PO Box 110, Budapest H-1325, Hungary

Ferenc Faigl and Elemér Fogassy

Research Group for Organic Chemical Technology, Hungarian Academy of Sciences, PO Box 91, Budapest H-1521, Hungary

Günther Reck

Institute of Molecular Biology, Academy of Sciences of the German Democratic Republic, Robert Rössler Strasse 10, Berlin-Buch 1115, DDR

The optical resolution of *trans*-3-(2,2-dichlorovinyl)-2,2-dimethylcyclopropanecarboxylic acid (**1**) with (*S*)-2-benzylaminobutanol (**2**) has been optimized. Thermodynamic constants, thermal behaviour, and the crystal structures of the diastereoisomeric salts were determined in order to evaluate the results of optical resolution. The resolving agent (**2**) exists in four different conformations in the diastereoisomeric salts of (**1**) and its *cis* isomer. The relative energies of these four rotamers have been studied by means of force-field calculations.

We earlier reported on the optical resolution of *cis*-3-(2,2-dichlorovinyl)-2,2-dimethylcyclopropanecarboxylic acid [*cis*-permethrinic acid] with (*S*)-2-benzylaminobutan-1-ol (**2**) as the resolving agent.<sup>1</sup> The pH dependence of the enantiomer separation, the thermodynamic constants, and the crystal structures of the two diastereoisomeric salts (SCPABA and RCPABA) were determined.

As the resolving agent (**2**) can easily be synthesised from a by-product of ethambutol (produced on a large scale as an antituberculosic), we tried to make use of it for the resolution of *trans*-permethrinic acid (**1**), as well. Some of the esters of (**1**) have significant insecticidal activity but they are less toxic towards mammals owing to their relatively high overall biodegradability.<sup>2</sup> 3-Phenoxybenzyl esters of the (+)-(1*R*)-*trans*-permethrinic acid are one order of magnitude more potent than the (-)-(1*S*)-isomer,<sup>3</sup> therefore the resolution of the *trans*-acid is important. In order to conduct more observations on the relationship between the physicochemical and structural parameters of the optical resolution,<sup>4</sup> we have determined the optimum parameters of the separation, the binary-phase diagram, the thermodynamic constants, and the crystal structure for both diastereoisomeric salts of (**2**) with (1*R*)-(**1**) (RTPABA) and (1*S*)-(**1**) (STPABA).

### Results and Discussion

The optimum circumstances for the resolution of (**1**) were determined by application of the thermodynamic equilibrium model<sup>5</sup> and the binary-phase diagrams of the diastereoisomeric salts. Our experience in the resolution of the *cis* isomer led us to study the separation of the *trans* acids primarily as a function of the pH. Figure 1 shows the results of resolution (solid lines), where the mole ratio of racemate to resolving agent was 2:1, while the amount of the achiral auxiliary reagent (NaOH) varied from 1 to 1.3 equiv. (related to the amount of the racemic acid). Without an excess of the base ([NaOH] = 1.0 equiv.) an approximately threefold abundance of the *R*-acid can be achieved in the almost quantitatively crystallizing diastereoisomeric salt (optical purity = 0.5); under the same conditions, we observed an optical purity of about 0.3 for the *cis* isomer. This is in accordance with the expected yield of separation based on the

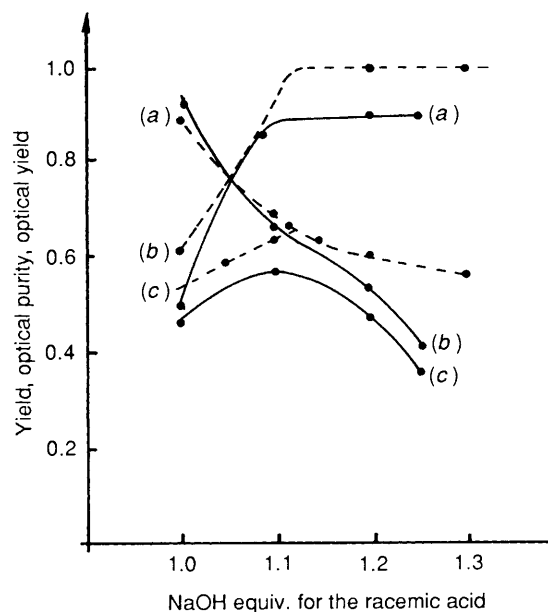


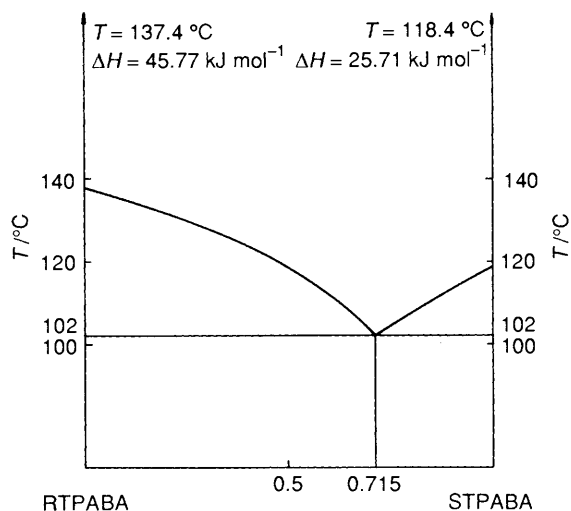
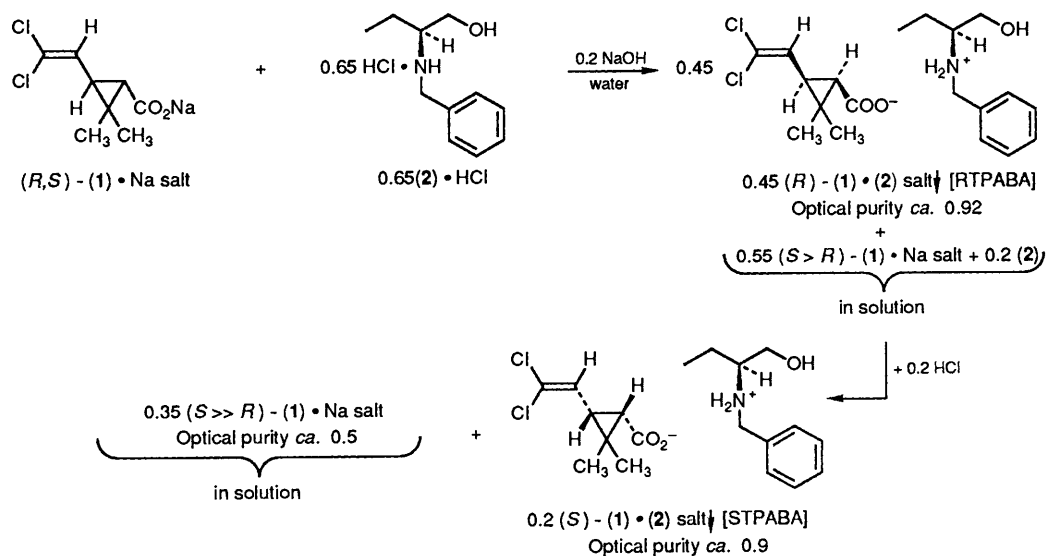
Figure 1. Changes in (a) optical purity, (b) yield, and (c) optical yield [= (a)  $\times$  (b)] of RTPABA with variation of the amount of sodium hydroxide during the optical resolution of *trans*-permethrinic acid: (—) measured; (---) calculated values.<sup>5</sup>

binary phase diagram (Figure 2), the eutectic composition  $E_u = 0.715$  corresponding to an optical purity of 0.45. Jacques *et al.*<sup>6</sup> and Ács *et al.*<sup>7</sup> observed that the eutectic composition is approximately equal to the eutonic composition of the above-mentioned stoichiometric mixture.

The improved optical yield is in accordance with the enhanced difference of the melting points and heats of fusion relative to the *cis* isomer. From the larger ratio of the solubility constant ( $K_{ss}/K_{sR} = 2.2$ ) and from the smaller ratio of the dissociation constants ( $K_{dS}/K_{dR} = 1.4$ ) (see Table 1), it is also to be expected that the degree of separation will be greater than in the case of the *cis*-isomer. The smaller slope of the curve as a function of the achiral auxiliary reagent (NaOH) is also due to

**Table 1.** Physicochemical parameters and crystal data.

Parameter	STPABA	RTPABA
Formulae	$C_{19}H_{27}Cl_2NO_3$	
$M_w$	388.3	
Solubility constant at 25 °C ( $K_s/mol\ dm^{-3}$ )	$2.27 \times 10^{-2}$	$1.04 \times 10^{-2}$
Dissociation constant at 25 °C ( $K_d/mol\ dm^{-3}$ )	$1.48 \times 10^{-4}$	$1.09 \times 10^{-4}$
M.p./°C	118.4	137.4
Heat of fusion, $\Delta H_m/kJ\ mol^{-1}$	25.71	45.77
$a/\text{Å}$	5.980(6)	6.100(1)
$b/\text{Å}$	8.436(2)	14.260(1)
$c/\text{Å}$	10.312(3)	11.681(2)
$\alpha/^\circ$	102.28(2)	
$\beta/^\circ$	91.75(5)	96.38(1)
$\gamma/^\circ$	93.24(5)	
$V/\text{Å}^3$	507.0	1 009.7
Space group	$P1$	$P2_1$
$Z$	1	2
$D_{calc}/g\ cm^{-3}$	1.20	1.28
$R$	0.067	0.051
$R_w$	0.072	0.054
$\mu/cm^{-1}$	3.29(Mo- $K_\alpha$ )	30.74(Cu- $K_\alpha$ )

**Figure 2.** Binary phase diagram of STPABA and RTPABA.**Scheme.****Table 2.** Selected torsion angles/°.

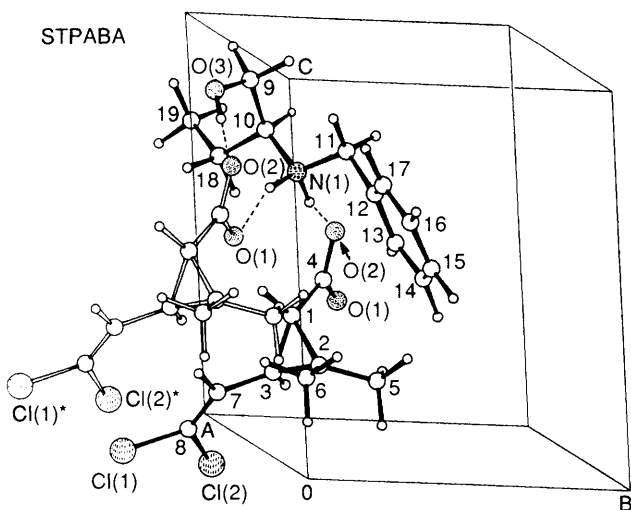
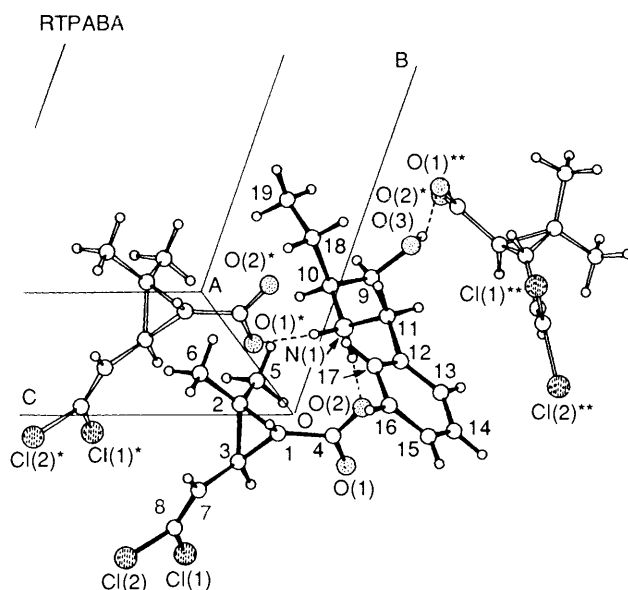
	STPABA	RTPABA
Anion		
C(8)–C(7)–C(3)–C(1)	153.7	–154.9
C(7)–C(3)–C(1)–C(4)	–135.9	137.1
C(3)–C(1)–C(4)–O(1)	–5.0	–7.1
Cation		
C(13)–C(12)–C(11)–N(1)	58.5	100.8
C(12)–C(11)–N(1)–C(10)	177.0	–177.5
C(11)–N(1)–C(10)–C(9)	–53.1	66.2
N(1)–C(10)–C(9)–O(3)	–63.4	–82.4
C(11)–N(1)–C(10)–C(18)	176.7	–63.0
N(1)–C(10)–C(18)–C(19)	–168.0	–166.4

the above facts. The dashed lines in Figure 1 show the values calculated on the basis of the thermodynamic equilibrium model;<sup>5</sup> the corresponding curves exhibit good agreement. The curve of the optical yield ( $S$ ) has a maximum at  $[NaOH] = 1.1$  equiv. The good optical yield in the presence of a small excess of the achiral auxiliary reagent (NaOH) is in accordance with the significant difference in melting points and heats of fusion (see Table 1). The efficiency of the optical separation could be further enhanced by increasing the amount of (2). The optimum values are shown in the reaction Scheme; with 0.65 equiv. (2) and 1.2 equiv. NaOH, the yield is 0.9, the optical purity is 0.92, and the optical yield ( $S$ ) is 0.82. As in the *cis* case, if the excess of NaOH in the mother liquor is neutralized with 2 mol  $dm^{-3}$  hydrochloric acid the other diastereoisomeric salt (STPABA) with relatively high optical purity (0.9) is precipitated, leaving a mother liquor corresponding to the eutectic composition of the acids ( $E_u = 0.45$ ). Accordingly, the observation of Jacques and co-workers that the isomeric ratio in the mother liquor corresponds to the eutectic composition of the binary phase diagram or to the eutonic composition of the ternary phase diagram is valid only if no excess of achiral acid or base is present in the reaction mixture.

**X-Ray Investigation.**—In order to find correlations between the solid-state structure, the physico-chemical data, and the resolution process, the crystal structures of the two diastereoisomeric salts were determined. As for the *cis* derivative, the less-

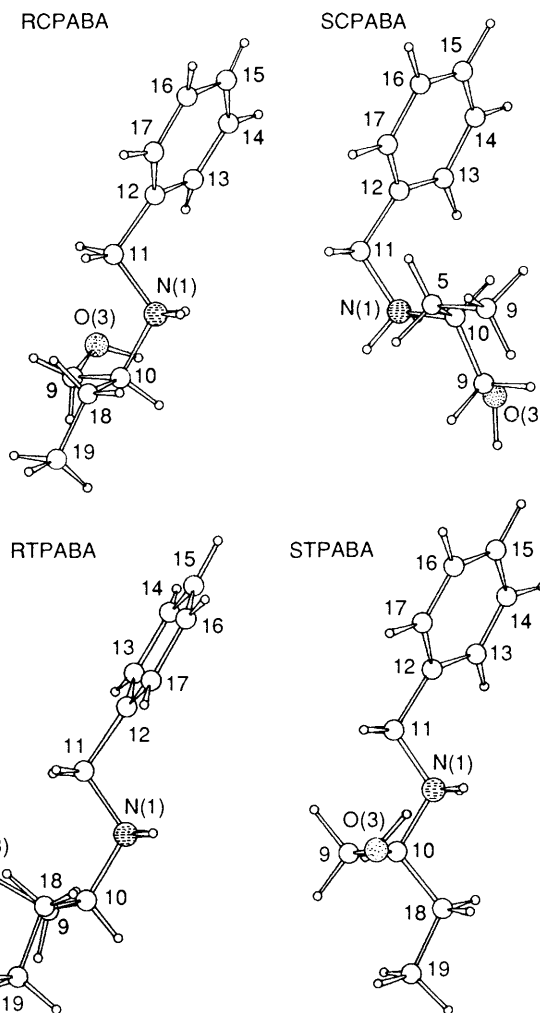
**Table 3.** N-H...O and O-H...O hydrogen bridges in the diastereoisomeric salts.

D-H...A	Symmetry	d/Å		
		D...A	H...A	D-H...A
<b>STPABA</b>				
N(1)-H(1N)...O(1)	[x + 1, y, z]	2.70	1.71	160
N(1)-H(2N)...O(2)	[x, y, z]	2.73	1.77	158
O(3)-H(O3)...O(2)	[x + 1, y, z]	2.71	1.71	180
<b>RTPABA</b>				
N(1)-H(1N)...O(2)	[x, y, z]	2.75	1.81	169
N(1)-H(2N)...O(1)	[x + 1, y, z]	2.76	1.82	170
O(3)-H(O3)...O(1)	[-x - 1, y + 0.5, -z]	2.75	1.85	149

**Figure 3.** Packing arrangement of STPABA.**Figure 4.** Packing arrangement of RTPABA.

soluble *trans* salt (RTPABA) crystallizes in the monoclinic  $P2_1$  space group, while the more soluble one (STBAPA) is triclinic, space group  $P1$  (Table 1), indicating that the more stable salt has the higher symmetry. The density difference is even more enhanced than in the *cis* case, in accordance with the thermodynamic data.

While the conformations of the anions in STPABA and

**Figure 5.** The four different rotamers of  $BAB^+$  found in the crystal structures of RCPABA, SCPABA, RTPABA, and STPABA. N(1), C(11), and C(12) are in the plane of the drawing in all cases.

RTPABA are approximately mirror-related (Table 2), those of the isochiral cations differ significantly around the N(1)-C(10) bond. In STPABA, atoms C(11) and C(18) of the benzyl and ethyl groups, respectively, are in the antiperiplanar position; in RTPABA the hydrogen atom attached to C(10) is antiperiplanar to C(11) [see also Figure 5(b)]. The position of the phenyl group also differs by about  $40^\circ$ . The rotamer relative to the C(10)-C(9) bond found in the STPABA structure is the most stable in solution.<sup>1</sup>

The hydrogen bonds are detailed in Table 3. The packing

**Table 4.** Comparison of the conformations and strain energies of different rotamers using the initial X-ray data (XRD) and force-field calculations (MMX) to minimize the strain energy of the cation and of the free base.

Torsion angle/°	RCPABA		SCPABA		STPABA		RTPABA	
	XRD	MMX	XRD	MMX	XRD	MMX	XRD	MMX
C(13)–C(12)–C(11)–N(1)								
Cation	67	65	58	65	59	82	101	99
Base		80		58		71		97
C(12)–C(11)–N(1)–C(10)								
Cation	–176	–177	48	48	177	–172	183	180
Base		180		55		–176		180
C(11)–N(1)–C(10)–C(9)								
Cation	52	58	178	–167	–53	–86	66	67
Base		60		–175		–67		69
N(1)–C(10)–C(9)–C(3)								
Cation	38	51	49	60	–63	–65	–82	–83
Base		52		56		–62		–84
N(1)–C(10)–C(18)–C(19)								
Cation	–175	–168	–179	–177	–168	–177	–166	–169
Base		–165		180		–175		–168
<i>E</i> /kcal mol <sup>–1</sup>								
Cation	41.6	15.3	43.5	14.3	49.2	14.6	50.2	15.2
Base	34.8	19.0	36.2	17.3	36.6	14.6	40.0	15.5

**Table 5.** Fractional co-ordinates for STPABA with esds values in parentheses.

Atom	x	y	z
Cl(1) (fixed)	0.1490	–0.5238	0.0295
Cl(2)	–0.270 0(5)	–0.380 7(5)	0.069 0(4)
O(1)	–0.254 1(8)	0.038 0(7)	0.488 3(5)
O(2)	0.049 3(8)	0.135 3(7)	0.616 5(5)
O(3)	0.873 4(10)	0.042 2(10)	0.829 7(8)
N(1)	0.494 3(9)	0.165 2(9)	0.692 7(6)
C(1)	0.100 4(10)	0.005 8(10)	0.392 0(7)
C(2)	0.090 1(10)	0.079 9(10)	0.271 3(7)
C(3)	0.001 4(10)	–0.090 8(9)	0.263 2(7)
C(4)	–0.042 1(10)	0.064 3(10)	0.507 8(7)
C(5)	–0.070 4(10)	0.206 4(10)	0.261 9(9)
C(6)	0.312 8(10)	0.107 3(10)	0.205 5(9)
C(7)	0.107 1(10)	–0.234 8(10)	0.192 0(8)
C(8)	0.017 0(10)	–0.358 7(10)	0.110 9(9)
C(9)	0.684 5(20)	0.093 9(20)	0.888 7(10)
C(10)	0.476 0(10)	0.070 0(10)	0.797 9(7)
C(11)	0.555 4(20)	0.340 1(10)	0.739 2(7)
C(12)	0.583 6(10)	0.429 8(10)	0.631 6(8)
C(13)	0.414 6(20)	0.435 6(10)	0.537 5(10)
C(14)	0.447 1(20)	0.524 9(10)	0.444 6(10)
C(15)	0.652 6(20)	0.615 7(10)	0.439 7(10)
C(16)	0.813 8(20)	0.607 3(10)	0.529 3(10)
C(17)	0.784 0(20)	0.519 5(10)	0.622 4(10)
C(18)	0.400 0(10)	–0.103 7(10)	0.737 8(9)
C(19)	0.329 2(20)	–0.205 2(10)	0.835 4(10)

**Table 6.** Fractional co-ordinates for RTPABA with esds values in parentheses.

Atom	x	y	z
Cl(1)	–0.653 1(2)	–0.130 3 (fixed)	0.414 8(1)
Cl(2)	–0.262 9(2)	–0.244 5(1)	0.427 5(1)
O(1)	–0.699 5(5)	0.073 8(2)	0.068 5(3)
O(2)	–0.424 4(5)	0.127 5(2)	–0.022 4(3)
O(3)	–0.127 5(6)	0.400 3(2)	–0.109 9(3)
N(1)	–0.006 8(6)	0.189 4(3)	–0.051 3(3)
C(1)	–0.329 0(7)	0.046 4(3)	0.150 5(3)
C(2)	–0.276 0(8)	0.095 7(4)	0.266 0(4)
C(3)	–0.401 4(7)	0.003 7(3)	0.260 9(4)
C(4)	–0.497 2(7)	0.085 3(3)	0.058 8(4)
C(5)	–0.407 0(10)	0.181 6(4)	0.291 3(5)
C(6)	–0.038 0(9)	0.098 2(5)	0.316 8(5)
C(7)	–0.299 9(8)	–0.084 7(4)	0.308 0(4)
C(8)	–0.394 0(8)	–0.143 3(4)	0.373 0(4)
C(9)	–0.178 0(8)	0.344 8(4)	–0.014 3(5)
C(10)	0.007 1(8)	0.277 6(3)	0.022 7(4)
C(11)	0.029 0(10)	0.205 3(4)	–0.174 1(4)
C(12)	0.002 5(8)	0.114 2(3)	–0.243 9(4)
C(13)	–0.191 5(9)	0.097 3(5)	–0.313 3(4)
C(14)	–0.205 0(10)	0.017 1(5)	–0.381 8(5)
C(15)	–0.031 0(10)	–0.041 6(5)	–0.383 5(5)
C(16)	0.160 0(10)	–0.024 2(5)	–0.315 2(5)
C(17)	0.179 0(9)	0.055 8(4)	–0.244 7(4)
C(18)	0.238 0(8)	0.320 2(4)	0.030 0(4)
C(19)	0.277 0(10)	0.392 7(4)	0.122 7(5)

arrangements are shown in Figure 3 and 4. In both structures, the two carboxylate oxygens participate in the salt-bridge formation, making a chain along the *a* axis. The hydrogen-bond system is completed by a third hydrogen bond between the hydroxy group and one of the carboxylate oxygens. In STPABA, this third hydrogen bond connects the same anion as one of the salt bridges [O(1)···H–N]; in RTPABA, a third

anion, generated by the twofold screw axis along the *b* axis, is involved, permitting a two-dimensional hydrogen-bond sheet perpendicular to the *c* axis.

Comparison of the crystal structures of the four diastereoisomeric salts (STPABA, RTPABA and their *cis* equivalents RCPABA and SCPABA) reveals that the cation of (2) (BAB) exists in four different conformations. In order to assess the

**Table 7.** Bond lengths for STPABA and RTPABA with esds in parentheses.

	STPABA	RTPABA
Cl(1)–C(8)	1.713(8)	1.715(5)
Cl(2)–C(8)	1.747(7)	1.736(6)
O(1)–C(4)	1.277(8)	1.262(5)
O(2)–C(4)	1.247(11)	1.246(5)
O(3)–C(9)	1.350(16)	1.430(6)
N(1)–C(10)	1.484(14)	1.523(6)
N(1)–C(11)	1.472(11)	1.492(6)
C(1)–C(2)	1.508(15)	1.524(6)
C(1)–C(3)	1.489(12)	1.535(5)
C(1)–C(4)	1.502(12)	1.505(5)
C(2)–C(3)	1.491(11)	1.516(7)
C(2)–C(5)	1.491(11)	1.510(8)
C(2)–C(6)	1.541(11)	1.507(7)
C(3)–C(7)	1.466(11)	1.483(7)
C(7)–C(8)	1.272(11)	1.304(7)
C(9)–C(10)	1.514(17)	1.507(7)
C(10)–C(18)	1.503(11)	1.528(7)
C(11)–C(12)	1.479(15)	1.533(7)
C(12)–C(13)	1.390(14)	1.379(7)
C(12)–C(17)	1.397(13)	1.362(7)
C(13)–C(14)	1.351(15)	1.393(10)
C(14)–C(15)	1.419(16)	1.354(9)
C(15)–C(16)	1.330(16)	1.360(8)
C(16)–C(17)	1.342(15)	1.404(9)
C(18)–C(19)	1.509(15)	1.497(7)

**Table 8.** Bond angles for SCPABA and RCPABA with esds in parentheses.

	STPABA	RTPABA
Cl(1)–C(8)–Cl(2)	110.6(5)	112.8(3)
Cl(1)–C(8)–C(7)	126.9(5)	125.1(4)
Cl(2)–C(8)–C(7)	122.5(6)	122.1(4)
O(1)–C(4)–O(2)	123.4(8)	124.5(4)
O(1)–C(4)–C(1)	117.1(7)	119.0(3)
O(2)–C(4)–C(1)	119.5(6)	116.6(4)
O(3)–C(9)–C(10)	115.3(14)	110.9(4)
N(1)–C(10)–C(9)	112.2(9)	111.7(3)
N(1)–C(10)–C(18)	110.2(7)	110.7(4)
C(10)–N(1)–C(11)	115.7(7)	114.5(4)
N(1)–C(11)–C(12)	114.3(8)	111.4(4)
C(1)–C(2)–C(3)	59.5(6)	60.6(3)
C(1)–C(2)–C(5)	120.6(7)	118.9(3)
C(1)–C(2)–C(6)	117.2(6)	117.4(4)
C(2)–C(1)–C(3)	59.7(6)	59.4(3)
C(2)–C(1)–C(4)	120.6(6)	121.4(4)
C(1)–C(3)–C(2)	60.8(6)	59.9(3)
C(1)–C(3)–C(7)	120.9(6)	120.1(4)
C(3)–C(1)–C(4)	121.7(5)	120.5(4)
C(2)–C(3)–C(7)	124.4(5)	122.2(4)
C(3)–C(2)–C(5)	119.1(5)	115.7(4)
C(3)–C(2)–C(6)	118.0(6)	119.7(4)
C(5)–C(2)–C(6)	112.8(8)	114.3(5)
C(3)–C(7)–C(8)	128.8(6)	124.6(5)
C(9)–C(10)–C(18)	115.5(9)	114.8(4)
C(10)–C(18)–C(19)	115.4(8)	112.7(4)
C(11)–C(12)–C(13)	123.2(7)	119.6(5)
C(11)–C(12)–C(17)	120.8(8)	119.0(4)
C(12)–C(13)–C(14)	120.5(10)	118.2(5)
C(13)–C(12)–C(17)	116.0(9)	121.1(5)
C(12)–C(17)–C(16)	122.7(10)	119.1(5)
C(13)–C(14)–C(15)	121.6(10)	121.3(5)
C(14)–C(16)–C(17)	117.2(9)	120.0(6)
C(15)–C(16)–C(17)	121.9(11)	120.1(6)

relative strain energies of these rotamers, energy minimization was performed with the MMX force-field program (an en-

hanced version of Allinger's MMPMI program<sup>8</sup>), using the X-ray co-ordinates as input geometry. As some of the force-field parameters for N<sup>+</sup> are either unknown or available only in generalized form, the same computations were done for the free base as well. The results are listed in Table 4. As concerns the five single bonds [C(12)–C(11), C(11)–N(1), N(1)–C(10), C(10)–C(9), and C(10)–C(18)], the conformation across the outer two [C(12)–C(11) and C(10)–C(18)] is approximately the same in all cases. Nevertheless, there is a significant deviation from the ideal value of 90° for the position of the phenyl group which is determined by the phenyl–ethyl and phenyl–hydroxy interactions. The C(19) methyl group is always in the anti-periplanar position. Accordingly, the conformation across the three inner single bonds determines the shape of the cation. Of the energetically different 18 rotamers with staggered conformation across the single bond,<sup>9</sup> four are involved in these structures. Taking the X-ray geometry, the lowest strain energy was found for BAB(RCPABA), and the highest one for the BAB(RTPABA) rotamer, for both the cation and the free base.

After minimization, the relative sequence of the energies found for the free base and for the cation differs, but nevertheless the molecules remain in the potential valley of the canonical conformer. For the free base BAB(STPABA) is the lowest-energy conformer, while for the cation it is BABH<sup>+</sup>(SCPABA). When the minimized energies are compared, the lower-energy conformer of BAB crystallizes in the more stable, less soluble salt (SCPABA) in the *cis* case, while the higher-energy conformer of BAB is found in the less soluble salt (RTPABA) in the *trans* case.

## Conclusions

Some resolving agents are built up from rigid rings (*e.g.* alkaloids<sup>10</sup>) or form stable chains.<sup>4</sup> In these cases the chiral recognition is based upon the interaction between the ions of the compounds to be resolved and the well-defined chiral surfaces of the resolving agent. We have studied another type of resolving agent, where the flexibility of the resolving base plays an important role, allowing the resolution of both *cis*- and *trans*-permethrinic acid with different conformations of the base in the solid state. Our force-field calculations have shown that the energy differences between the four rotamers are small, and thus intermolecular contacts can easily overcompensate them. The most striking observation is that the strain energy of BAB(RTPABA) is higher than that of BAB(STPABA) according to any type of calculation (cation or free base, X-ray geometry or optimized one).

As the melting point and heat of fusion differences are more enhanced in the *trans* case than in the *cis* case, it can be concluded that mostly the intermolecular contacts determine the crystal-lattice energies, overcompensating the slight energy difference between the rotamers.

The accumulation of structural and physicochemical data on diastereoisomeric salts might form the basis of a rational design of the most suitable resolving agent for a given racemate. Our present investigation has shown that the conformational flexibility of the resolving agent has also to be taken into account while making predictions for the structure and behaviour of diastereoisomeric salts.

## Experimental

Thermal data were recorded with the DSC cell of the Dupont 1090 TA system. Potentiometric titration was performed with a Radelkis precision pH-meter with a combined glass electrode. Optical rotational power was measured by means of a Perkin-Elmer 241 polarimeter.

*Optical Resolution of trans-Permethrinic Acid.*—Racemic (1) (20.9 g, 0.1 mol) was dissolved at 80–90 °C in water (150 cm<sup>3</sup>) containing sodium hydroxide (4.8 g, 0.12 mol). The clear solution was treated with (2) (11.6 g, 0.065 mol) dissolved in hydrochloric acid (1 mol dm<sup>-3</sup>; 65 cm<sup>3</sup>; 0.065 mol). The mixture was allowed to cool to room temperature. The resulting precipitate was the salt (2) of (1R) (1) (RTPABA) (17.4 g, m.p. 137 °C).

The mother liquor was neutralized by addition of hydrochloric acid (2 mol dm<sup>-3</sup>; 10 cm<sup>3</sup>; 0.02 mol) with stirring. After a while the salt (2) of (1S) (1) (STPABA) precipitated out (7.7 g, m.p. 118 °C).

Optically active (1) could be obtained by decomposing the diastereoisomeric salts with 2 mol dm<sup>-3</sup> hydrochloric acid. The free acids precipitated out {9.4 g *R*-isomer,  $[\alpha]_D^{22} = +36.3^\circ$  ( $c = 1$ , CHCl<sub>3</sub>); 4.1 g *S*-isomer,  $[\alpha]_D^{22} = -35.5^\circ$  ( $c = 1$ , in CHCl<sub>3</sub>)}.

*X-Ray Investigation.*—Crystals of STPABA and RTPABA were grown from methanol and acetone, respectively. Crystal data are listed in Table 1. Data on RTPABA were collected on an Enraf-Nonius CAD-4 diffractometer with monochromated Cu-K<sub>α</sub> radiation (at the Central Research Institute for Chemistry of the Hungarian Academy of Sciences, Budapest). 2 179 independent reflections ( $2\theta_{\max} = 150^\circ$ ) were collected. The intensity reduction of 7% was corrected by means of intensity standard reflections. The structure was solved through the application of the MULTAN 84 program. The reliability factor for the positions of non-hydrogen atoms after isotropic refinement decreased to  $R = 0.13$ . An empirical absorption correction was applied to all reflections, using the DIFABS<sup>11</sup> program ( $R = 0.10$ ). After anisotropic refinement, the reliability factor was  $R = 0.051$ ,  $R_w = 0.054$  for 1973 reflections [ $I > 3\sigma(I)$ ,  $p = 0.04$ ]. Hydrogen atoms with known positions were generated, except for N–H, O–H, H(1) and H(3) were taken from difference Fourier calculations. The fractional co-ordinates with their esd values are given in Table 5.\*

Data on STPABA were also collected on a CAD-4 diffractometer with monochromated Mo-K<sub>α</sub> radiation at the Institute of Physical Chemistry of the Academy of Sciences of the GDR, Berlin. 1 769 independent reflections were obtained. The structure was solved with the MULTAN 84 program. No

absorption correction was applied. Hydrogen atoms with known positions were generated; hydrogen atoms attached to N and O atoms or to the ring were taken from the electron density difference map. Anisotropic refinement concluded with  $R = 0.066$ ,  $R = 0.071$  for 1 619 reflections [ $I > 3\sigma(I)$ ,  $p = 0.01$ ]. The fractional co-ordinates with their esd values are listed in Table 6.

Bond lengths and bond angles for the non-hydrogen atoms are given in Tables 7 and 8, respectively.

Structure determinations were carried out on a PDP 11/34 minicomputer by means of the Enraf-Nonius SDP program package with local modifications. The weighting scheme was  $w = 1/[\sigma^2(F_o) + PF_o^2]$ . Force-field calculations were performed on an IBM-AT compatible personal computer.

### Acknowledgements

We are grateful to Dr. Gy. Pokol, Institute of General and Analytical Chemistry, and to Dr. M. Ács, Department of Organic Chemical Technology, Technical University, Budapest for the DSC measurements and discussions.

### References

- 1 E. Fogassy, F. Faigl, M. Ács, K. Simon, É. Kozsda, B. Podányi, M. Czugler, and G. Reck, *J. Chem. Soc., Perkin Trans. 2*, 1988, 1385.
- 2 D. M. Soderlund, J. E. Casida, in 'Synthetic Pyrethroids,' ACS Symp. Ser. 42, ed. M. Elliott, Washington, 1977, p. 173.
- 3 P. E. Burt, M. Elliott, A. W. Farnham, N. F. Janes, P. H. Needham, *Pestic. Sci.*, 1974, 5, 791.
- 4 E. Fogassy, M. Ács, F. Faigl, K. Simon, J. Rohonczy, and Z. Ecsery, *J. Chem. Soc., Perkin Trans. 2*, 1986, 1881.
- 5 E. Fogassy, F. Faigl, M. Ács, A. Grofcsik, *J. Chem. Res.*, 1981 (S) 346; (M) 3981.
- 6 J. Jacques, A. Collet, and S. H. Wilen, 'Enantiomers, Racemates and Resolutions,' Wiley, New York, 1981.
- 7 M. Ács, Gy. Pokol, F. Faigl, and E. Fogassy, *J. Therm. Anal.*, 1988, 33, 1241.
- 8 N. L. Allinger, MMPMI program (QCPE 395), Dept. of Chemistry, University of Georgia, 1986.
- 9 W. Klyne and K. Prelog, *Experientia*, 1960, 16, 521.
- 10 R. O. Gould, R. Kelly, and M. D. Walkinshaw, *J. Chem. Soc., Perkin Trans. 2*, 1985, 847.
- 11 N. Walker and D. Stuart, *Acta Crystallogr., Sect. A*, 1983, 39, 158.

\* Full lists of bond angles, bond lengths, and thermal parameters have been deposited at the Cambridge Crystallographic Data Centre. For details of the CCDC deposition scheme, see 'Instructions for Authors (1990),' *J. Chem. Soc., Perkin Trans. 2*, 1990, issue 1.